

**18th International Conference on
Harmonisation within Atmospheric Dispersion Modelling for Regulatory Purposes
9-12 October 2017, Bologna, Italy**

**LAGRANGIAN TIME SCALES OF THE TURBULENCE ABOVE TWO-DIMENSIONAL
CANOPIES**

Annalisa Di Bernardino¹, Paolo Monti¹, Giovanni Leuzzi¹, Fabio Sammartino¹ and Giorgio Querzoli²

¹DICEA, Università di Roma “La Sapienza”, Via Eudossiana 18, Rome, Italy

²Dipartimento di Ingegneria del Territorio, Università di Cagliari, Italy

Abstract: Lagrangian statistics are obtained from a water-channel experiment of an idealized two-dimensional urban canopy flow in neutral conditions. The objective is to quantify both the streamwise and vertical components of the Lagrangian time scale of the turbulence (T_u^L and T_w^L , respectively) above the canopy as well as to investigate their dependence on the aspect ratio of the canopy, AR, as the latter is the ratio of the width (W) to the height (H) of the canyons constituting the canopy. It is found that T_w^L follows Raupach’s linear law within the constant flux layer in both the canopies analysed (AR=1 and AR=2). The same holds true for T_u^L but only when AR=1, while for AR=2 it follows Raupach’s law for $z>2H$ (here z is the height). Below that level, T_u^L is nearly constant with height, showing at $z=H$ a value approximately one order of magnitude greater than the one found for AR=1.

Key words: *Autocorrelation function; Building; Feature tracking; Raupach law; Urban canopy; Water channel.*

INTRODUCTION

The interest in determining the Lagrangian time scale of the turbulence (T^L) in atmospheric flows stems from the fact that it is one of the main parameters involved in Lagrangian models of turbulent dispersion (Thomson, 1987). These can be easily coupled with common Reynolds-averaged Navier-Stokes (RANS) models, which have gained a growing interest owing to their relatively small computational cost (e.g. Badas et al., 2017). RANS models, however, do not compute the Lagrangian time scale that must be estimated from parametric laws founded on theoretical bases and generally applicable only to simple cases (e.g. flat terrain). Theoretical predictions of T^L valid on complex terrain are not known (e.g. Amicarelli et al., 2011). On the other hand, its experimental determination is not simple, especially in the case of complex geometry, when the flow strongly varies in space.

Under neutral conditions, two-dimensional canopy flows can be classified based on the aspect ratio. For $AR \leq 1.5$ (skimming flow) a single vortex develops inside the canyon; for $1.5 \leq AR \leq 2.5$ (wake interference regime) the flow pattern is more complex and two counter-rotating vortices form; for higher AR values the distance between the buildings is so long that each obstacle does not affect the others (isolated obstacle regime). Even the flow above the canopy layer depends strongly on AR. In fact, for $AR \leq 1.5$ the flow has difficulty in penetrating the interelement spaces and therefore it skims, remaining nearly parallel to the roofs (Grimmond and Oke, 1999). In contrast, for the wake interference regime the interaction between canyon and upper flow is considerable and the roughness sub-layer (RSL) tends to be thicker (Pelliccioni et al., 2016).

The Lagrangian time scale is defined as the time integral of the velocity autocorrelation function, ρ^L , viz.,

$$T_L = \int_0^{\infty} \rho^L d\tau \quad (1)$$

and gives a rough measure of the time taken by a fluid particle to become decorrelated with its initial state (here τ is the time lag). The present experiments allowed the detection of particle trajectories long enough

to permit the calculation of the autocorrelation function. Eulerian quantities, such as mean velocity, velocity variance and the vertical momentum flux are also determined. Two experimental arrangements are considered for the analysis. The first uses an arrays of obstacles simulating two-dimensional canyons with aspect ratio $AR=1$, while for the second arrangement AR is equal to 2. For this scope, a neutral atmospheric boundary layer has been simulated in the water channel. Velocities were measured using a technique based on the image analysis.

EXPERIMENTAL SETUP

The experiments are performed using a closed-loop water-channel facility (Figure 1; details on the experimental apparatus can be found in Di Bernardino et al., 2015a). The channel is 0.35 m high, 0.25 m wide, 7.40 m long, and a constant head reservoir feeds the flume. A floodgate allows regulating the water depth and, therefore, the water velocity. A series of parallelepipeds (made by black PVC) of square section $B=H=2$ cm and length equal to the channel width are glued onto the channel bottom (Figure 2).

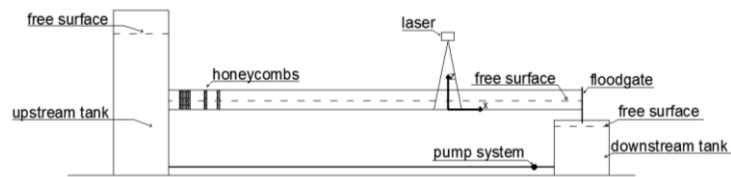


Figure 1. Side view of the experimental apparatus. The x-axis refers to the longitudinal axis of the channel, while the z-axis is parallel to the vertical.

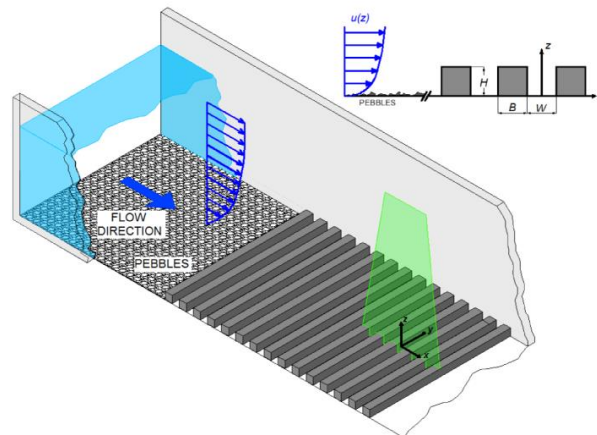


Figure 2. Sketch of the modelled street canyon. The vertical plane in green represents the laser beam.

With the aim of recreating both the vertical profile of the wind velocity and the nearly-constant vertical flux of momentum typically observed in real atmospheric surface layers on flat terrain, the roughness of the channel bottom upstream of the buildings is increased by means of randomly distributed pebbles (average diameter ≈ 5 mm), glued onto the surface (Figure 2). The water depth and the freestream velocity are 0.16 m and $U=0.33$ m s^{-1} , respectively. The Reynolds number based on obstacle height and on the average velocity at $z=H$ is nearly 3800, while the one based on the friction velocity, $u_* = \sqrt{-u'w'}$, i.e. $Re_\tau = u_*H/\nu$, varies from 390 to 470 (u and w are the streamwise and the vertical velocity components, prime is the fluctuation around the mean, indicated with bar, and $\nu=10^{-2}$ cm² s⁻¹ is the kinematic viscosity of water). Therefore, Re is well above the critical value and, consequently, the simulated large-scale structures can be considered as being independent of Re (fully rough wall regime, see Snyder (1972). Additional information on the Re independence of the flow are reported in Di Bernardino et al. (2015b)).

The area considered for the measurements of the Eulerian variables is rectangular, lying in the vertical x - z plane parallel to the streamwise direction and passing through the centre of the channel (Figure 1). A thin laser light sheet (2 mm thick) from a 5 W green laser beam passing through a cylindrical lens

illuminates the measurement plane. The water is seeded with neutrally buoyant particles (2 μm in diameter), which are assumed as being transported passively by the flow. The framed area, 60 mm long (x-axis) and 60 mm high (z-axis), is located 30 buildings downstream of the first building so as to minimize any influence from the change in roughness between the pebbles and the building array. A set of images is taken during each experiment by means of a high-speed video camera at 250 Hz (1280x1024 pixels resolution) for a sampling interval of 40 s. Velocity measurements are performed using a feature tracking technique that recognizes particle trajectories by means of a dedicated algorithm. With this technique, individual particle trajectories are illuminated throughout a volume of the flow and tracked using the camera. A Gaussian interpolation algorithm (Monti et al., 2007) is applied at each time instant to the scattered velocity samples on the x-z plane to obtain the instantaneous Eulerian description of the velocity field over a regular 120x120 array. After this procedure, 10000 velocity fields with 0.5 mm spatial resolution and 1/250 s temporal resolution are obtained. Following the assessment of the repeatability of the conditions by performing the same experiment several times, a second series of experiments is run in the same condition described above in order to track the particle trajectories for the evaluation of the Lagrangian statistics. The illumination and acquisition set-up is tailored with the aim of acquiring trajectories as long as possible. The region framed by the high-speed camera is 0.20 m in width and is illuminated by a light sheet 20 mm thick generated by a 1000 W, halogen lamp. Each run lasts for 120 s and nearly 200000 trajectories are available for calculating the Lagrangian time scale.

The statistics of the Eulerian velocity fields are obtained by time averaging over $Nt=10000$ acquired time instants at each grid node of the 120x120 array. The Lagrangian time scales are calculated from the set of particle trajectories detected during the image-processing procedure. In particular,

$$T_j^L(\underline{x}_0) = \int_0^{\infty} \rho_j^L(\underline{x}_0, \tau) d\tau \quad (2)$$

where, provided the phenomenon is statistically steady in a Eulerian sense:

$$\rho_j^L(\underline{x}_0, \tau) = \frac{1}{M_{\underline{x}_0}} \frac{\sum_{k|\underline{x}_0} \left\{ U_j^{(k)}(\underline{x}_0, \tau) - \langle U_j \rangle(\underline{x}_0, \tau) \right\} \left[U_j^{(k)}(\underline{x}_0, 0) - \langle U_j \rangle(\underline{x}_0, 0) \right]}{\sigma_j^L(\underline{x}_0, \tau) \sigma_j^L(\underline{x}_0, 0)} \quad (3)$$

Here, \underline{x}_0 indicates the reference position of the k-th particle (underscore indicates vector quantities, $j=1,2,3$ the axis of the reference frame, $\langle \rangle$ the Lagrangian average), $M_{\underline{x}_0}$ the number of trajectories starting from \underline{x}_0 , $U_j^{(k)}$ the velocity, while σ_j^L is the standard deviation of the j-th component of the velocity (for more explanation about equation 3 see Di Bernardino et al., 2017).

RESULTS

The vertical profiles of the Eulerian variables above the canopy are determined by adopting the canopy approach (e.g. Finnigan 2000), i.e. by horizontally averaging the time averaged statistics over a region including one building top and the contiguous canyon. In doing so, the results can be assumed as representative of the repeating unit constituting the canopy. Figure 3 shows the normalized streamwise velocity and $\overline{u'w'}$ measured for AR=1 and 2. In the latter case, $\overline{u'w'}$ is higher everywhere and shows values close to its maximum over a deeper layer. This is reasonable in that the larger vertical mixing caused by the stronger interaction between the outer flow and the underlying cavity occurring for AR=2, as a result of the larger drag exerted by the roughness elements, makes the constant-flux layer thicker, causing the lowering of the streamwise velocities.

The autocorrelations ρ_u^L and ρ_w^L are calculated following all the trajectories that begin in a horizontal fluid layer 1 mm thick, extended horizontally over the whole domain, passing through each of the nodes of the Eulerian grid. The corresponding Lagrangian time scales, T_u^L and T_w^L , are determined by using equation 2 by considering the time lag at which the autocorrelations decrease to 1/e (e.g. Anfossi et al., 2006). For AR=1, ρ_u^L and ρ_w^L do not show considerable differences, and both decrease more slowly at higher levels (Figure 4). The same is valid for ρ_w^L when AR=2, while ρ_u^L , in contrast, appears to be less

sensitive to the height, particularly close to the roof top. The considerable dependence of ρ_u^L on AR is apparent by looking at the vertical profiles of T_u^L and T_w^L (Figure 5), made non-dimensional by the time scale $H/u_{*,ref}$ ($u_{*,ref}$ is the reference friction velocity, i.e. the average of u_* calculated over the height range where u_* is nearly constant, see Figure 3).

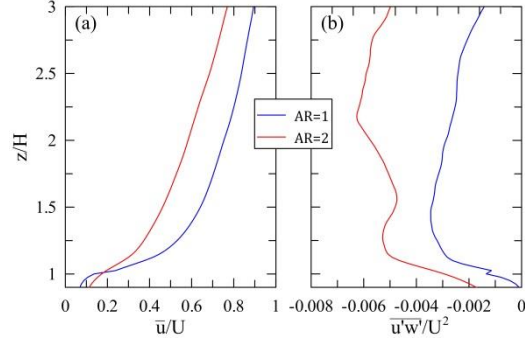


Figure 3. Vertical profiles of (a) streamwise velocity and (b) Reynolds stress for AR=1 (blue) and AR=2 (red).

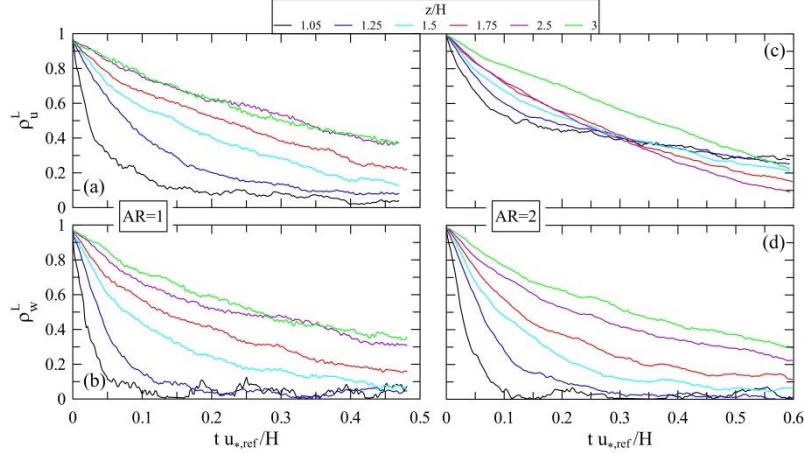


Figure 4. (a) Streamwise and (b) vertical components of the Lagrangian autocorrelation functions calculated at different distance from the canopy top ($z/H=1$) for AR=1. (c) and (d) as (a) and (b), but for AR=2. The values of the reference friction velocities are $u_{*,ref}=19.5 \text{ mm s}^{-1}$ and 24.5 mm s^{-1} for AR=1 and 2, respectively.

In essence, the Lagrangian time scale calculated for the streamwise velocity component (blue dots in Figure 5) shows a strong qualitative and quantitative dependence on the aspect ratio, i.e. larger values of T_u^L occur for AR=2 above the canopy top compared to AR=1. In this case, both T_u^L and T_w^L grow more or less linearly with height for the whole boundary layer investigated, while the former for AR=2 is constant in the whole RSL as well as for a considerable portion of the constant flux layer. Then, it grows roughly linearly with height for $z>2H$ where, quite surprisingly, $T_u^L \approx T_w^L$. In contrast, the two T_w^L do not change appreciably with AR. Note that the growth of T_w^L with the height is in reasonable agreement with the linear law (continuous line in Fig. 5, Raupach 1989):

$$\frac{T_w^L u_{*,ref}}{H} = \frac{k}{\left([\sigma_w/u_{*,ref}]\right)^2} \frac{z-d}{H} \quad (4)$$

obtained by matching the expression of the linear growth with the height of the eddy diffusivity of momentum based on the Prandtl mixing length theory and the far-field eddy diffusivity (Taylor, 1921). The quantity $d=0.9H$ and $0.77H$ in equation 4 is the displacement height for AR=1 and 2, respectively, obtained using the parametric law proposed by Kastner-Klein and Rotach (2004). It is worthwhile stressing here that Eq. (4) has been used in the past only for vegetation canopies (e.g. Leuning et al. 2000) and, to our knowledge, this is the first time it has been tested in urban canopy layers.

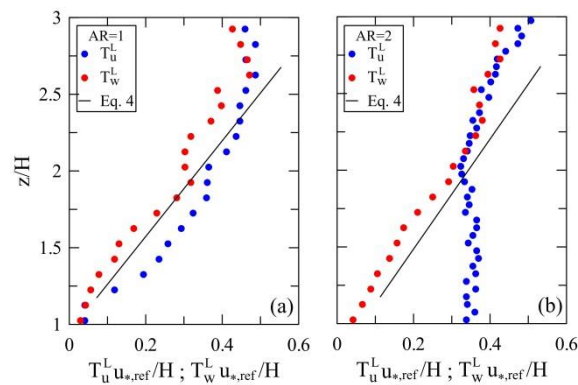


Figure 5. Vertical profiles of the non-dimensional Lagrangian time scales estimated for (a) AR=1 and (b) AR=2.

CONCLUSIONS

A water-channel facility has been used to measure the Lagrangian time scale of the turbulence above an array of two-dimensional square rods simulating idealized urban flows for two different aspect ratios (AR=1 and 2) of the canopy. The results show a certain dependence of the streamwise component of the time scale on AR. Further work remains to be done to understand whether the behaviours seen above hold true also for other aspect ratios of the canopy.

REFERENCES

- Amicarelli, A., G. Leuzzi, P. Monti, D.J. Thomson, 2011: A comparison between IECM and IEM models, *Int. J. Environ. Pollut.*, **47**, 324-331.
- Anfossi, D., U. Rizza, C. Mangia, G. A. Degrazia and E. Pereira Marques Filho, 2006: Estimation of the ratio between the Lagrangian and Eulerian time scales in an atmospheric boundary layer generated by large eddy simulation. *Atmos. Environ.*, **40**, 326-337.
- Badas, M. G., S. Ferrari, M. Garau and G. Querzoli, 2017: On the effect of gable roof on natural ventilation in two-dimensional urban canyons. *J. Wind Eng. Ind. Aerod.*, **162**, 24-34.
- Di Bernardino, A., P. Monti, G. Leuzzi and G. Querzoli, 2015a: A laboratory investigation of flow and turbulence over a two-dimensional urban canopy. *Boundary-Layer Meteorol.*, **155**, 73-85.
- Di Bernardino, A., P. Monti, G. Leuzzi and G. Querzoli, 2015b: On the effect of the aspect ratio on flow and turbulence over a two-dimensional street canyon. *Int. J. Environ. Pollut.*, **58**, 27-38.
- Di Bernardino, A., P. Monti, G. Leuzzi and G. Querzoli, 2017: Water-channel estimation of Eulerian and Lagrangian time scales of the turbulence in idealized two-dimensional urban canopies. *Boundary-Layer Meteorol.*, **165**, 251-276.
- Finnigan, J., 2000: Turbulence in plant canopies. *Annu. Rev. Fluid Mech.*, **32**, 519-571.
- Grimmond, C. S. B. and T. R. Oke, 1999: Aerodynamic properties of urban areas derived from analysis of urban surface form. *J. Appl. Meteorol.*, **38**, 1261-1292.
- Kastner-Klein, P. and M. W. Rotach, 2004: Mean flow and turbulence characteristics in an urban roughness sublayer. *Boundary-Layer Meteorol.*, **111**, 55-84.
- Leuning, R., O.T. Denmead, A. Miyata and J. Kim, 2000: Source/sink distributions of heat, water vapour, carbon dioxide and methane in a rice canopy estimated using Lagrangian dispersion analysis. *Agric. For. Meteorol.*, **104**, 233-249.
- Monti, P., G. Querzoli, A. Cenedese and S. Piccinini, 2007: Mixing properties of a stably stratified parallel shear layer. *Phys. Fluids.*, **19**:085104 (1-9). DOI: 10.1063/1.2756580.
- Pelliccioni, A., P. Monti and G. Leuzzi, 2016: Wind-speed profile and roughness sublayer depth modelling in urban boundary layers. *Boundary-Layer Meteorol.*, **160**, 225-248.
- Raupach, M. R., 1989: Applying Lagrangian fluid mechanics to infer scalar source distributions from concentration profiles in plant canopies. *Agric. For. Meteorol.*, **47**, 85-108.
- Snyder, W. H., 1972: Similarity criteria for the application of fluid models to the study of air pollution meteorology. *Boundary-Layer Meteorol.*, **3**, 113-134.
- Taylor, G. I., 1921: Diffusion by continuous movements. *Proc. Lond. Math. Soc.*, **20**, 196.
- Thomson, D. J., 1987: Criteria for the selection of stochastic models of particle trajectories in turbulent flows. *J. Fluid Mech.*, **180**, 529-556.